This is a preprint, the final version is subject to change, of the American Mineralogist (MSA)
Cite as Authors (Year) Title. American Mineralogist, in press.
DOI: https://doi.org/10.2138/am-2018-6329

Revision 1

Segerstromite, $Ca_3(As^{5+}O_4)_2[As^{3+}(OH)_3]_2$, the first mineral containing the $As^{3+}(OH)_3$ arsenite molecule, from the Cobriza mine in the Atacama Region, Chile.

Hexiong Yang*, Robert T. Downs, Robert A. Jenkins, Stanley H. Evans
Department of Geosciences, University of Arizona, Tucson, Arizona 85721-0077, U.S.A.

Corresponding author: hyang@email.arizona.edu

Abstract

A new mineral species, segerstromite, ideally $Ca_3(As^{5+}O_4)_2[As^{3+}(OH)_3]_2$, has been discovered at the Cobriza mine in the Sacramento district in the Copiapó Province, Chile. Crystals of segerstromite occur as tetrahedra or dodecahedra (up to 0.50 × 0.50 × 0.50 mm), or in blocky aggregates. Associated minerals include talmessite, vladimirite, and Sr-bearing hydroxylapatite. Similar to the associated minerals, segerstromite is a secondary mineral. The new mineral is colorless in transmitted light, transparent with white streak and vitreous luster. It is brittle and has a Mohs hardness of ~4.5. No cleavage, parting, or twinning was observed. The measured and calculated densities are 3.44(3) and 3.46 g/cm^3, respectively. Optically, segerstromite is isotropic, with n = 1.731(5). It is insoluble in water or hydrochloric acid. An electron microprobe analysis yielded an empirical formula (based on 14 O apfu) $Ca_{2.98}(AsO_4)_{2.00}[As(OH)_3]_{2.00}$.

Segerstromite is cubic, with space group $I2_13$ and unit-cell parameters a = 10.7627(2) Å, V = 1246.71(4) Å^3, and Z = 4. Its crystal structure is constructed from three different polyhedral units: distorted CaO_8 cubes, rigid $As^{5+}O_4$ arsenate tetrahedra, and neutral $As^{3+}(OH)_3$ arsenite triangular pyramids. The Ca-groups form layers of corrugated crankshaft chains that lie parallel to the cubic axes. These chains are linked by the isolated $As^{5+}O_4$ and $As^{3+}(OH)_3$ groups. Segerstromite is the first known crystalline

compound that contains the $As^{3+}(OH)_3$ arsenite molecule, pointing to a new potential approach to remove highly toxic and mobile $As^{3+}(OH)_3$ from drinking water.

***Key words*:** new mineral, segerstromite, arsenate/arsenite, crystal structure, X-ray diffraction, Raman spectrum

Introduction

A new mineral species, segerstromite, ideally $Ca_3(As^{5+}O_4)_2[As^{3+}(OH)_3]_2$, has been found at the Cobriza mine in the Sacramento district in the Copiapó Province, Atacama Region, Chile. It is named in honor of the late Kenneth Segerstrom (1909-1992), who was a professional geologist and worked more than 40 years for the U.S. Geological Survey in the U.S., Mexico and Chile, principally conducting field-based regional geologic studies. In particular, Ken Segerstrom worked in Chile in conjunction with the "Instituto de Investigaciones Geologicas" (now Sernageomin), from 1957-1963, mainly in the Atacama Region, where the new mineral was found. Among his numerous publications, Ken Segerstrom authored 18 maps and articles on the Atacama Region, including the Sacramento district and the Cobriza mine. The new mineral and its name have been approved by the Commission on New Minerals, Nomenclature and Classification (CNMNC) of the International Mineralogical Association (IMA 2014-001). Part of the cotype sample has been deposited at the University of Arizona Mineral Museum (Catalogue # 19800) and the RRUFF Project (deposition # R130753).

Arsenic contamination can be a major ecological hazard because of its well-known toxicity and carcinogenicity, even at very low concentrations in drinking water (10 μg/L) (Hughes 2002; Vaughan 2011). In natural water, arsenic primarily exists in inorganic forms with two predominant species: $H_3As^{3+}O_3$ arsenite [or commonly written as $As^{3+}(OH)_3$] and $H_3As^{5+}O_4$ arsenate. The toxicity of arsenic depends strongly on its oxidation state, with As^{3+} 25-60 times more toxic than As^{5+} (Fazal et al. 2001). Although

some sophisticated methods have been developed to remove As^{5+} from drinking water, such as by ion-exchange, adsorption, or as a precipitate of $AlAsO_4$ or $FeAsO_4$, there is no efficient or economic approach to eliminate As^{3+} as yet, due partly to its greater solubility and mobility than As^{5+} (e.g., Zhang et al. 2007; Mohan and Pittman 2007; Itakura et al. 2008; Kreidie et al. 2011; Roy et al. 2016; Dickson et al. 2017; Yadav et al. 2017). Extensive efforts, both experimental and theoretical, have been devoted to seek ligands that can form stable complexes with $As^{3+}(OH)_3$ and some successes have been achieved with certain organic compounds (e.g., Porquet and Filella 2007; Kolozsi et al. 2008). Nonetheless, there has been no report for the presence of the $As^{3+}(OH)_3$ group in any inorganic crystalline material, synthetic or natural, until now. Therefore, segerstromite represents the first inorganic compound that sequesters the $As^{3+}(OH)_3$ group in its structure.

Sample Description and Experimental Methods

Occurrence, physical and chemical properties, and Raman spectra

Segerstromite was found on several specimens collected by RAJ from the Cobriza mine (27°49'45"S, 70°14'03"W) in the Sacramento district in the Copiapó Province, Atacama Region, Chile. The Cobriza mine is an abandoned Pb-Ag-As-Cu-Zn mine; the mineralization is hosted in sedimentary and volcanic rocks.

Crystals of segerstromite occur as tetrahedra, dodecahedra, granular or blocky aggregates, with single crystals up to 0.50 x 0.50 x 0.50 mm (Fig 1). Associated minerals include talmessite $Ca_2Mg(AsO_4)_2 \cdot 2H_2O$, vladimirite $Ca_4(AsO_4)_2(AsO_3OH) \cdot 4H_2O$, and Sr-bearing hydroxylapatite $Ca_5(PO_4)_3(OH)$. Similar to the other associated minerals (talmessite and vladimirite), segerstromite is considered to be a secondary mineral. Vladimirite from the Cobriza mine has been previously investigated by Yang et al. (2011).

Segerstromite is colorless in transmitted light, transparent with white streak and vitreous luster. It is brittle and has a Mohs hardness of ~4.5; no cleavage, parting, or twinning was observed. The measured (by flotation) and calculated densities are 3.44(3) and 3.46 g/cm^3, respectively. Optically, segerstromite is isotropic, with n = 1.731(5), measured in white light. It is insoluble in water or hydrochloric acid.

The chemical composition of segerstromite was determined using a CAMECA SX-100 electron microprobe (WDS mode, 10 kV, 6 nA, and 10 μm beam diameter). The standards included As_2O_3 for As, and wollastonite ($CaSiO_3$) for Ca, yielding an average composition (wt.%) (16 points) of As_2O_3 60.75(16) [converted to As_2O_3 30.38 + As_2O_5 35.20 with As^{3+}/As^{5+} = 1 according to the X-ray structure determination, see below], CaO 25.57(12), H_2O 8.29 (added according to the structure determination), and total = 99.53(26). The resultant chemical formula, calculated on the basis of 14 O *apfu* (from the structure determination), is $Ca_{2.98}(AsO_4)_{2.00}[As(OH)_3]_{2.00}$, which can be simplified to $Ca_3(As^{5+}O_4)_2[As^{3+}(OH)_3]_2$.

The Raman spectrum of segerstromite was collected on a randomly oriented crystal on a Thermo Almega microRaman system, using a solid-state laser with a frequency of 532 nm and a thermoelectric cooled CCD detector. The laser is partially polarized with 4 cm^{-1} resolution and a spot size of 1 μm.

X-ray crystallography

Both the powder and single-crystal X-ray diffraction data for segerstromite were collected on a Bruker X8 APEX2 CCD X-ray diffractometer equipped with graphite-monochromatized MoK_α radiation. Listed in Table 1 are the measured powder X-ray diffraction data, along with those calculated from the determined structure using the program XPOW (Downs et al. 1993).

Single-crystal X-ray diffraction data of segerstromite were collected from a nearly equidimensional crystal (0.05 x 0.04 x 0.04 mm) with frame widths of 0.5° in ω and 30 s

counting time per frame. All reflections were indexed on the basis of a cubic unit-cell (Table 2*) (deposited). The intensity data were corrected for X-ray absorption using the Bruker program SADABS. The systematic absences of reflections suggest possible space group $I23$, $I2_13$, or $Im3$. The crystal structure was solved and refined using SHELX2014 (Sheldrick 2015a, 2015b) based on space group $I2_13$, because it produced the better refinement statistics in terms of bond lengths and angles, atomic displacement parameters, and *R* factors. The H atom was located from the difference Fourier maps. The ideal chemistry was assumed during the refinements. The positions of all atoms were refined with anisotropic displacement parameters, except those for the H atom, which was refined with an isotropic parameter. Final coordinates and displacement parameters of atoms in segerstromite are listed in Table 3, and selected bond-distances in Table 4* (deposited). Calculated bond-valence sums using the parameters from Brese and O'Keeffe (1991) are given in Table 5.

Discussion

Crystal structure

The crystal structure of segerstromite is unique. It is constructed from three different polyhedral units: distorted CaO_8 cubes with six short and two long Ca-O bonds, rigid $As^{5+}O_4$ arsenate tetrahedra, and neutral $As^{3+}(OH)_3$ arsenite triangular pyramids (**Table 3 and Fig. 2**). The $As^{5+}O_4$ and $As^{3+}(OH)_3$ groups are isolated from each other, while the Ca-groups form corrugated crankshaft chains that layer perpendicular to the cubic axes (**Fig. 3**). The corrugations are stabilized by the $As^{3+}(OH)_3$ arsenite groups. The layers are stacked with a shift of half a unit cell, so that the chains lie above and below the gaps between the chains (**Fig. 4**). The corrugated layers are held together by chains of CaO_8 groups linked by the isolated AsO_4 arsenate groups (**Fig. 5**).

There are a number of minerals that contain both As^{5+} and As^{3+} (Table 6), but segerstromite is the first known crystalline compound that contains the neutral $As^{3+}(OH)_3$

arsenite group. The average As^{3+}-O bond length for the $As^{3+}(OH)_3$ group is 1.776 Å, in excellent agreement with the experimental value of 1.77-1.78 Å reported for the $As^{3+}(OH)_3$ molecule in aqueous solutions (Arai et al. 2001; Pokrovski et al. 2002; Ramirez-Solis et al. 2004; Testamale et al. 2004). It also falls in the range between 1.77 and 1.82 Å calculated by various theoretical methods (see Porquet and Filella 2007; Tossell and Zimmermann, 2008; Hernández-Cobos et al. 2010). The O-As^{3+}-O angle is 95.29°, with a trigonal pyramidal lone-pair-As^{3+}-O angle of 121.43°.

The $As^{5+}O_4$ tetrahedron is slightly distorted, with the As1-O1 bond length (1.698 Å) longer than the three As1-O2 distances (1.679 Å) (Table 3). The average As^{5+}-O bond length is 1.684 Å, in accord with the values found in many other arsenate minerals (Hawthorne et al. 2012; Kampf et al. 2015; Đorđević et al. 2016 and references therein), as well as the average value of 1.685 Å derived by Majzlan et al. (2014) through an examination of numerous arsenate minerals.

The hydrogen bonding scheme in segerstromite is presented in Table 3. The O3—H…O2 distance is 2.664(2) Å, indicating a considerably strong hydrogen bond.

Raman spectrum

Numerous Raman spectroscopic studies have been conducted on various arsenite and/or arsenate minerals and compounds (e.g., Frost et al. 2011; Kharbish 2012; Liu et al. 2014; Đorđević 2015; Đorđević et al. 2016, and references therein), as well as on the $As(OH)_3$ molecule in organic materials and solutions (e.g., Loehr and Plane 1968; Pokrovski et al. 1999; Goldberg and Johnston 2001; Wood et al. 2002; Müller et al. 2010). The Raman spectrum of segerstromite is displayed in Figure 6 and the tentative assignments of major Raman bands based on the previous studies are given in Table 7. In particular, the bands at 699 and 680 cm^{-1} are ascribed to the symmetric and asymmetric stretching vibrations of As-OH within the $As^{3+}(OH)_3$ group, respectively, which should be compared with 701-710 and 655-669 cm^{-1} observed for the $As(OH)_3$ group in aqueous

solutions (Loehr and Plane 1968; Pokrovski et al. 1999; Goldberg and Johnston 2001; Müller et al. 2010).

In Figure 6, the O-H stretching vibration is marked by a rather broad band at 2906 cm^{-1}. According to Libowitzky (1999), an O—H…O distance of 2.66 Å would correspond to an O—H stretching frequency of ~2900 cm^{-1}, consistent with our measured value. Similar results were also reported for diaspore, which has an O—H…O distance of 2.65 Å with the O—H…O angle of 160.8° (Hill 1979) and a Raman band at 2918 cm^{-1} that is attributable to the O-H stretching vibration (Ruan et al. 2001).

Implications

In comparison to As^{5+}, besides its greater toxicity, $As^{3+}(OH)_3$ is also more mobile and soluble in the environment because of its neutral character in a wide pH range (<9.2 at 25 °C with As = 0.1 mol/L) (Müller et al. 2010), resulting in its rather weaker adsorption on soil constituents, such as iron and aluminum oxy-hydroxides (Ladeira and Ciminelli 2004; Yokoyama et al. 2012). All previous investigations have appeared to focus chiefly on the understanding of how $As^{3+}(OH)_3$ can be immobilized with the formation of complexes with Fe^{3+} and Al^{3+}. In particular, the possibility of co-precipitation of As^{3+} and Fe^{3+} has been explored extensively, because such a phenomenon has been observed to take place in natural environments, as well as under laboratory conditions (e.g., Ciardelli et al., 2008; Sasaki et al., 2009; Muller et al. 2010). Recently, Itakura et al. (2007, 2008) proposed the removal of arsenic from water containing both arsenite and arsenate ions through hydrothermal formation of the mineral johnbaumite, $Ca_5(As^{5+}O_4)_3(OH)$ (arsenate analogue of apatite). The discovery of segerstromite, however, points to a new potential approach to remove or reduce $As^{3+}(OH)_3$ in water, providing sufficient availability of Ca^{2+}. Because calcite, $CaCO_3$, is the most stable polymorph of calcium carbonates under the ambient conditions and ubiquitously found in various surface environments, a potential chemical reaction for such a process would be:

$$3CaCO_3 \text{ (calcite)} + 2H_3As^{5+}O_4\ (l) + 2H_3As^{3+}O_3\ (l) <===>$$

$$Ca_3(As^{5+}O_4)_2[As^{3+}(OH)_3]_2 \text{ (segerstromite)} \downarrow + 3H_2O + CO_2\uparrow$$

Hence, further investigations on the formation conditions of segerstromite, such as pH, Eh, and temperature, will undoubtedly generate information on how to remove $As^{3+}(OH)_3$ in water more efficiently and economically.

Acknowledgements

This study was funded by the Science Foundation Arizona. The constructive comments by Anthony R. Kampf and an anonymous reviewer are greatly appreciated.

References Cited

Arai, Y., Elzinga, E.J., and Sparks, D. (2001) X-ray absorption spectroscopic investigation of arsenite and arsenate adsorption at the aluminum oxide-water interface. Journal of Colloid and Interfacial Science, 235, 80-88.

Brese, N.E. and O'Keeffe, M. (1991) Bond-valence parameters for solids. Acta Crystallographica, B47, 192–197.

Ciardelli, M.C., Xu, H., and Sahai, N. (2008) Role of Fe(II), phosphate, silicate, sulfate, and carbonate in arsenic uptake by coprecipitation in synthetic and natural groundwater. Water Research, 42, 615-624.

Dickson, D., Liu, G, Cai, Y. (2017) Adsorption kinetics and isotherms of arsenite and arsenate on hematite nanoparticles and aggregates. Journal of Environmental Management, 186, 261-267.

Đorđević, T. (2015) Crystal Chemistry of the $M1^{1+,2+}$-$M2^{2+,3+}$–H-arsenites: the first cadmium(II) arsenite, $Na_4Cd_7(AsO_3)_6$. Zeitschrift fur Anorganische und Allgemeine Chemie, 641, 1863-1868.

Đorđević, T., Kolitsch, U., and Nasadala, L. (2016) A single-crystal X-ray and Raman spectroscopic study of hydrothermally synthesized arsenates and vanadates with

the descloizite and adelite structure types. American Mineralogist, 101, 1135-1149.

Downs, R.T., Bartelmehs, K.L., Gibbs, G.V. and Boisen, M.B., Jr. (1993) Interactive software for calculating and displaying X-ray or neutron powder diffractometer patterns of crystalline materials. American Mineralogist, 78, 1104-1107.

Fazal, M.A., Kawachi, T., amd Ichion, E. (2001) Extent and Severity of Groundwater Arsenic Contamination in Bangladesh. Water International, 26, 370–379.

Frost, R.L., Čejka, J., Sejkora, J., Plášil, J., Bahfenne, S., and Keeffe, E.C. (2011): Raman spectroscopy of hydrogen arsenate group $(AsO_3OH)_2$ in solid-state compounds: cobalt-containing zinc arsenate mineral, koritnigite $(Zn,Co)(AsO_3OH)•H_2O$. Journal of Raman Spectroscopy, 42, 534-539.

Goldberg, S. and Johnston, C.T. (2001) Mechanisms of arsenic adsorption on amorphous oxides evaluated using macroscopic measurements, vibrational spectroscopy, and surface complexation modeling. Journal of Colloid and Interfacial Science, 234, 204–216.

Hawthorne, F.C., Cooper, M.A., Abdu, Y.A., Ball, N.A., Back, M.E., and Tait, K.T. (2012) Davidlloydite, ideally $Zn_3(AsO_4)_2(H_2O)_4$, a new arsenate mineral from the Tsumeb mine, Otjikoto (Oshikoto) region, Namibia: description and crystal structure. Mineralogical Magazine, 76, 45-57.

Hernández-Cobos, J., Cristina Vargas, M., Ramírez-Solís, A. and Ortega-Blake, I. (2010) Aqueous solvation of $As(OH)_3$: A Monte Carlo study with flexible polarizable classical interaction potentials. The Journal of Chemical Physics, 133, 114501(1-9).

Hill, R.J. (1979) Crystal structure refinement and electron density distribution in diaspore, Physics and Chemistry of Minerals, 5, 179-200.

Hughes, M. F. (2002) Arsenic toxicity and potential mechanisms of action. Toxicology Letter, 133, 1-16.

244 Itakura, T., Sasai, R., and Itoh, H. (2007) Arsenic recovery from water containing
245 arsenite and arsenate ions by hydrothermal mineralization. Journal of Hazardous
246 Materials, 328–333.
247 Itakura, T., Sasai, R., and Itoh, H. (2008) A precipitation method for arsenite ion in
248 aqueous solution as natural mineral by hydrothermal mineralization. Journal of
249 the Ceramic Society of Japan, 116, 234-238.
250 Kampf, A.R., Mills, S.J., Nash, B.P., Dini, M., and Donoso, A.A.M. (2015) Tapiaite,
251 $Ca_5Al_2(AsO_4)_4(OH)_4 \cdot 12H_2O$, a new mineral from the Jote mine, Tierra Amarilla,
252 Chile. Mineralogical Magazine, 79, 345-354.
253 Kharbish, S. (2012) Raman spectra of minerals containing interconnected $As(Sb)O_3$
254 pyramids: trippkeite and schafarzikite. Journal of Geosciences, 57, 53-62.
255 Kolozsi, A., Lakatos, A., Galbács, G., Madsen, A. Ø., Larsen, E., and Gyurcsik, B.
256 (2008) A pH-Metric, UV, NMR, and X-ray Crystallographic Study on Arsenous
257 Acid Reacting with Dithioerythritol. Inorganic Chemistry, 47, 3832-3840.
258 Kreidie, N., Armiento, G., Cibin, G., Cinque, G., Crovato, C., Nardi, E., Pacifico, R.,
259 Cremisini, C., and Mottana, A. (2011) An integrated geochemical and
260 mineralogical approach for the evaluation of arsenic mobility in mining soils.
261 Journal of Soils and Sediments, 11, 37–52.
262 Ladeira, A.C.Q., Ciminelli, V.S.T. (2004) Adsorption and desorption of arsenic on an
263 oxisol and its constituents. Water Research, 38, 2087-2094.
264 Libowitzky, E. (1999) Correlation of O-H stretching frequencies and O-H···O hydrogen
265 bond lengths in minerals. Monatshefte für Chemie, 130, 1047-1059.
266 Liu, J., Jia, R., Liu, J. (2014) The vibration characterization of synthetic crystalline lead
267 hydrogen arsenite chloride precipitates $Pb_2(HAsO_3)Cl_2$-implications of
268 solidification of As (III) and Pb (II). Spectrochimica Acta Part A: Molecular and
269 Biomolecular Spectroscopy, 117, 658–661.
270 Loehr, T.M. and Plane, R.A. (1968) Raman spectra and structures of arsenious acid and

arsenites in aqueous solution. Inorganic Chemistry, 7, 1708–1714.

Majzlan, J., Drahota, P., Filippi, M. (2014) Parageneses and crystal chemistry of arsenic minerals. Reviews in Mineralogy and Geochemistry, 79, 17-184.

Mohan, D. and Pittman, C.U. Jr. (2007) Arsenic removal from water/wastewater using adsorbents—A critical review. Journal of Hazardous Materials, 142, 1–53.

Müller, K., Ciminelli, V.S.T., Dantas, M.S.S., and Willscher, S. (2010) A comparative study of As(III) and As(V) in aqueous solutions and adsorbed on iron oxy-hydroxides by Raman spectroscopy. Water Research, 44, 5660-5672.

Porquet, A. and Filella, M. (2007) Structural Evidence of the Similarity of $Sb(OH)_3$ and $As(OH)_3$ with Glycerol: Implications for Their Uptake. Chemical Research of Toxicology, 20, 1269–1276.

Pokrovski, G.D., Bény, J-M., and Zotov, A. (1999) Solubility and Raman spectroscopic study of As(III) speciation in organic compound-water solutions. A hydration approach for aqueous arsenic in complex solutions. Journal of Solution Chemistry, 28, 1307-1327.

Pokrovski, G.S., Zakirov, I., Roux, J., Testemale, D., Hazemann, J.-L., Bychkov, A. Yu., and Golikova, G.V. (2002) Experimental study of arsenic speciation in vapor phase to 500 °C: implications for As transport and fractionation in low-density crustal fluids and volcanic gases. Geochimica et Cosmochimica Acta, 66, 3453–3480.

Ramirez-Solis, A., Mukopadhyay, R., Rosen, B.P., and Stemmler, T.L. (2004) Experimental and theoretical characterization of arsenite in water: insights into the coordination environment of As-O. Inorganic Chemistry, 43, 2954–2959.

Roy, E., Patra, S., Rashmi Madhuri, R., Sharma, P.K. (2016) A single solution for arsenite and arsenate removal from drinking water using cysteine@ZnS:TiO_2 nanoparticle modified molecularly imprinted biofouling-resistant filtration membrane. Chemical Engineering Journal, 304, 259–270.

298 Ruan, H.D., Frost, R.L., Kloprogge, J.T. (2001) Comparison of Raman spectra in
299 characterizing gibbsite, bayerite, diaspore and boehmite, Journal of Raman
300 Spectroscopy, 32, 745-750.
301 Sasaki, K., Nakano, H., Wilopo, W., Miura, Y., Hirajima, T. (2009) Sorption and
302 speciation of arsenic by zero-valent iron. Colloids and Surfaces A:
303 Physicochemical Engineering Aspects, 347, 8-17.
304
305 Sheldrick, G. M. (2015a) SHELXT – Integrated space-group and crystal structure
306 determination. Acta Crystallographica, A71, 3-8.
307 Sheldrick, G. M. (2015b) Crystal structure refinement with SHELX. Acta
308 Crystallographica, C71, 3-8.
309 Testamale, D., Hazemann, J.-L., Pokrovski, G.S., Joly, Y., Roux, J., Argoud, R., and
310 Geaymond, O. (2004) Structural and electronic evolution of the $As(OH)_3$
311 molecule in high temperature aqueous solutions: an X-ray absorption
312 investigation. Journal of Chemical Physics, 121, 8973–8982.
313 Tossell , J.A. and Zimmermann, M.D. (2008) Calculation of the structures, stabilities, and
314 vibrational spectra of arsenites, thioarsenites and thioarsenates in aqueous solution.
315 Geochimica et Cosmochimica Acta, 72, 5232–5242.
316 Vaughan, D.J. (2011) Arsenic. Elements, 2, 71-75.
317 Wood, S.A., Tait, C.D., and Janecky, D.R. (2002) A Raman spectroscopic study of
318 arsenite and thioarsenite species in aqueous solution at 25 °C. Geochemical
319 Transactions, 3, 31–39.
320 Yadav, M.K., Gupta, A.K., Ghosal, P.S., Mukherjee, A. (2017) pH mediated facile
321 preparation of hydrotalcite based adsorbent for enhanced arsenite and arsenate
322 removal: Insights on physicochemical properties and adsorption mechanism.
323 Journal of Molecular Liquids, 240, 240–252
324 Yang, H., Evans, S.H., Downs, R.T., Jenkins, R.A. (2011) The crystal structure of
325 vladimirite, with a revised chemical formula, $Ca_4(AsO_4)_2(AsO_3OH)\cdot 4H_2O$. The
326 Canadian Mineralogist, 49, 1055-1064.
327 Yokoyama, Y., Kazuya Tanaka, K., Takahashi, Y. (2012) Differences in the

328 immobilization of arsenite and arsenate by calcite. Geochimica et Cosmochimica
329 Acta, 91, 202–219.
330 Zhang, G., Qu, J., Liu, H., Liu, R., and Li, G. (2007) Removal Mechanism of As(III) by a
331 Novel Fe−Mn Binary Oxide Adsorbent: Oxidation and Sorption. Environmental
332 Science & Technology, 41, 4613-4619.

333

List of Tables

List of Figure Captions

Figure 1a

Figure 1b

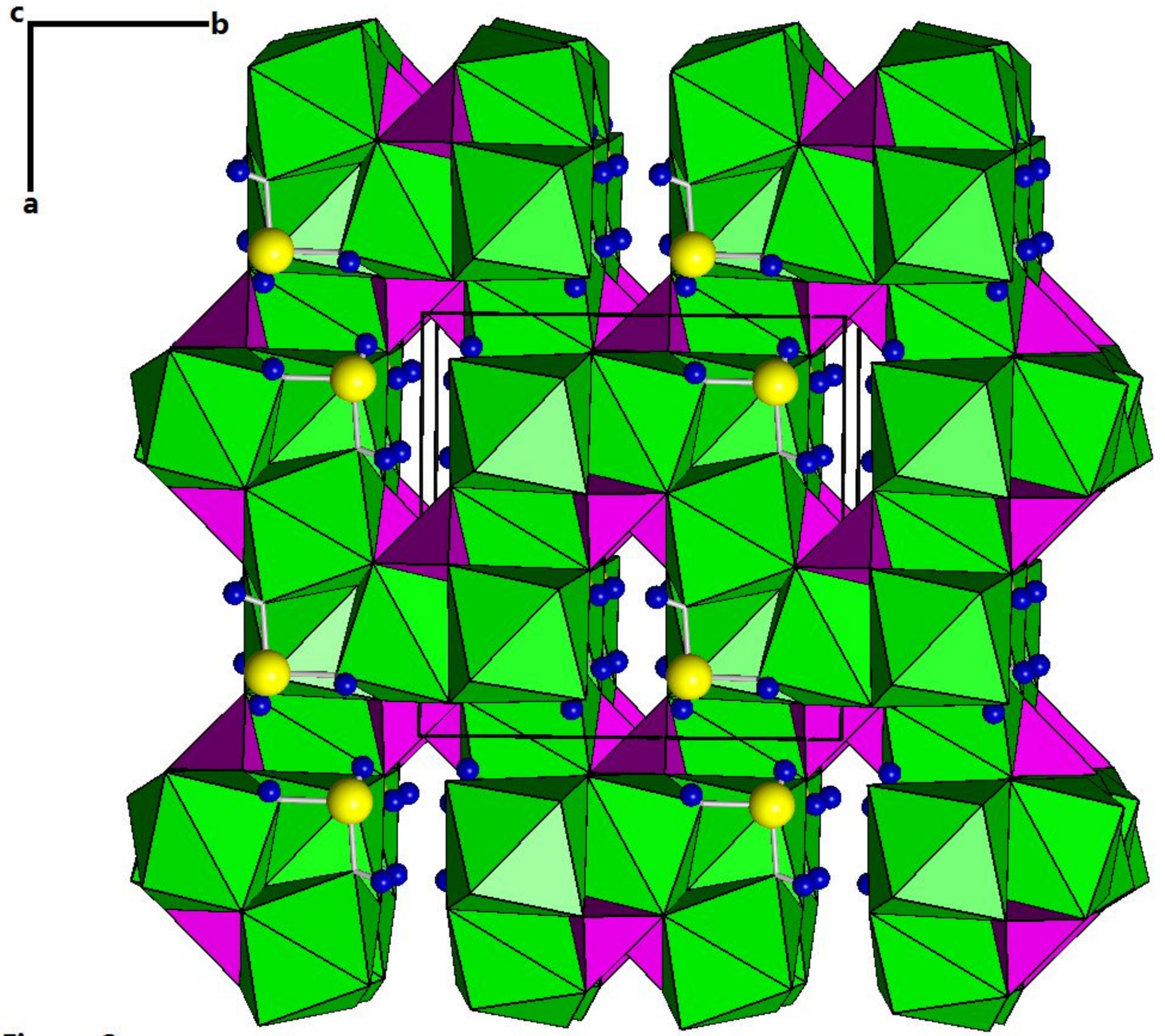

Figure 2

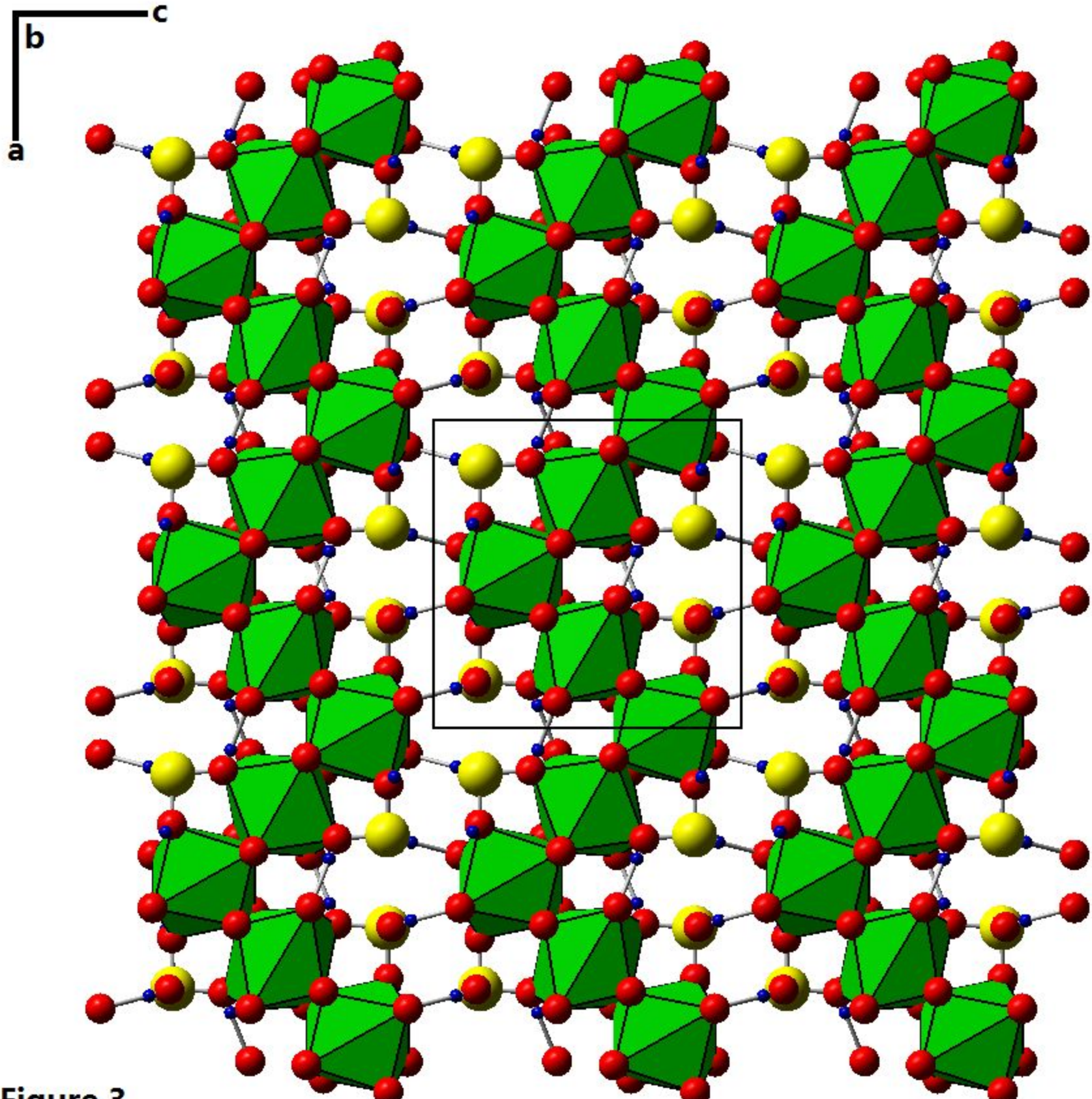

Figure 3

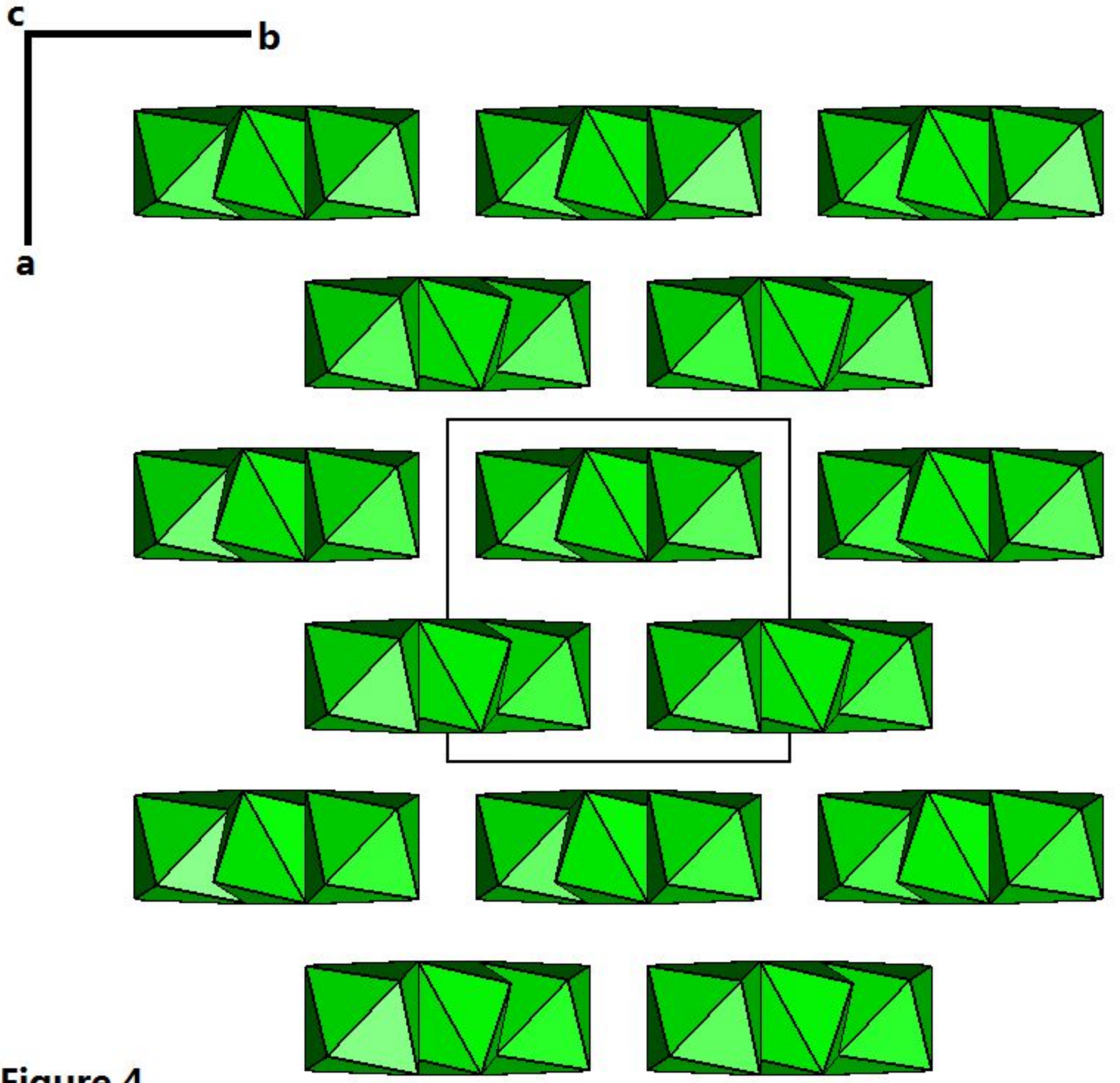

Figure 4

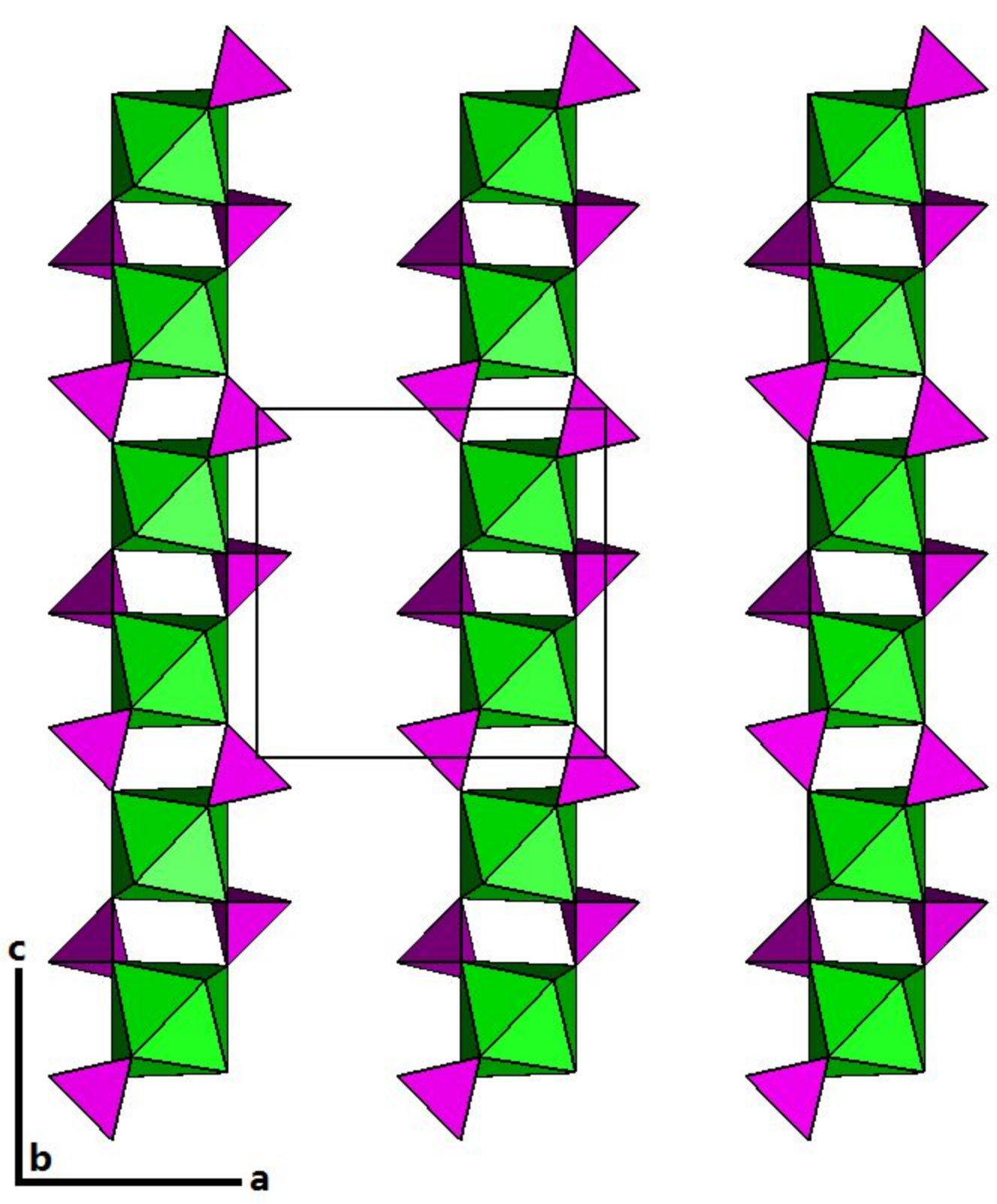

Figure 5

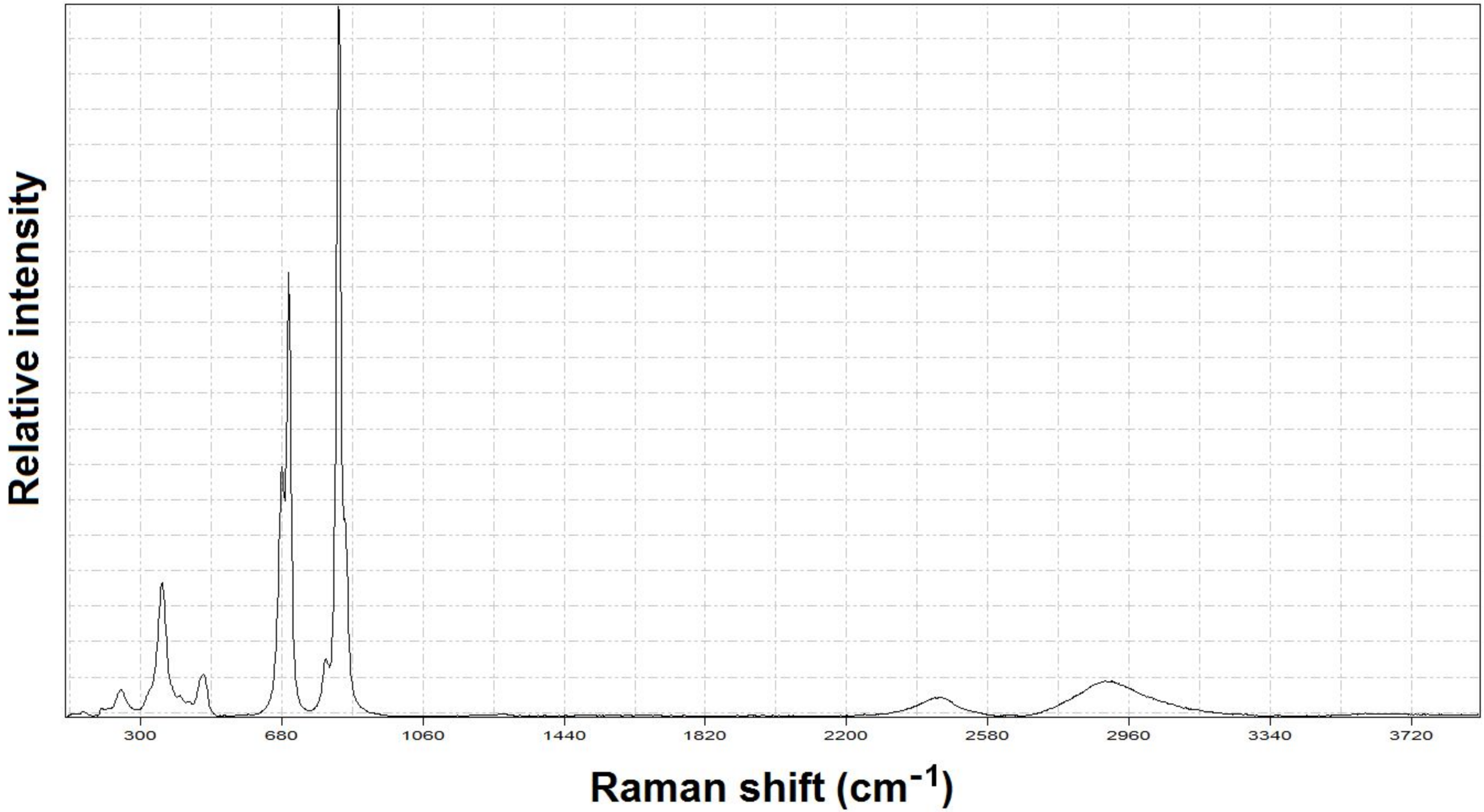
Relative intensity
300
680
1060
1440
1820
2200
2580
2960
3340
3720
Raman shift (cm-1)

Figure 6

Table 1. Powder diffraction data for segerstromite

Experimental		Theoretical				
INTENSITY	D-SPACING	INTENSITY	D-SPACING	H	K	L
34	4.351	8.52	4.3939	2	1	1
25	3.775	28.74	3.8052	2	2	0
82	3.389	77.54	3.4035	3	0	1
		22.46	3.4035	3	1	0
33	3.104	39.94	3.1069	2	2	2
100	2.875	16.47	2.8765	3	2	1
		77.46	2.8765	3	1	2
7	2.691	27.58	2.6907	4	0	0
14	2.536	13.93	2.5368	4	1	1
		7.08	2.2946	3	3	2
		27.77	2.1969	4	2	2
		5.24	2.1107	4	3	1
45	2.111	32.87	2.1107	5	1	0
7	1.965	8.86	1.9650	5	2	1
27	1.905	44.44	1.9026	4	4	0
34	1.748	8.16	1.7459	5	3	2
		17.10	1.7459	6	1	1
		4.84	1.7459	5	2	3
11	1.703	10.50	1.7017	6	2	0
		14.73	1.7017	6	0	2
16	1.663	8.67	1.6607	5	4	1
7	1.624	5.00	1.6225	6	2	2
13	1.588	3.39	1.5869	6	3	1
		12.25	1.5869	6	1	3
12	1.524	4.84	1.5221	5	3	4
19	1.465	8.63	1.4646	7	1	2
		9.08	1.4646	7	2	1
		3.05	1.4646	6	3	3

Table 2. Crystal data and refinement results for segerstromite.

Ideal chemical formula	$Ca_3(As^{5+}O_4)_2[As^{3+}(OH)_3]_2$
Crystal symmetry	Cubic
Space group	$I2_13$
a(Å)	10.7627(2)
V(Å^3)	1246.71(4)
Z	4
ρ_{cal}(g/cm^3)	3.44(3)
λ (Å, Mo$K\alpha$)	0.71073
μ (mm^{-1})	11.938
2θ range for data collection	≤65.18
No. of reflections collected	5985
No. of independent reflections	768
No. of reflections with $I > 2\sigma(I)$	747
No. of parameters refined	38
R(int)	0.028
Final R_1, wR_2 factors [$I > 2\sigma(I)$]	0.010, 0.020
Final R_1, wR_2 factors (all data)	0.011, 0.020
Goodness-of-fit	0.921

Table 4. Coordinates and displacement parameters of atoms in segerstromite

Atom	*x*	*y*	*z*	U_{eq}	U_{11}	U_{22}	U_{33}	U_{23}	U_{13}	U_{12}
Ca	0.22040(3)	0.5	0.25	0.01067(8)	0.01174(18)	0.01055(17)	0.00971(17)	0.00269(13)	0	0
As1	0.45009(1)	0.54991(1)	0.04991(1)	0.00677(6)	0.00677(6)	0.00677(6)	0.00677(6)	0.00067(5)	-0.00067(5)	-0.00067(5)
As2	0.15093(1)	0.15093(1)	0.15093(1)	0.00954(6)	0.00954(6)	0.00954(6)	0.00954(6)	-0.00049(5)	-0.00049(5)	-0.00049(5)
O1	0.3590(1)	0.6410(1)	0.1410(1)	0.0126(3)	0.0126(3)	0.0126(3)	0.0126(3)	-0.0026(4)	0.0026(4)	0.0026(4)
O2	0.4150(1)	0.5862(1)	0.9023(1)	0.0141(2)	0.0167(5)	0.0173(5)	0.0082(4)	0.0045(4)	-0.0048(4)	-0.0050(4)
O3	0.1480(1)	0.3155(1)	0.1384(1)	0.0147(2)	0.0208(5)	0.0096(5)	0.0137(5)	0.0018(4)	-0.0027(5)	0.0013(4)
H	0.127(2)	0.339(2)	0.073(2)	0.036(6)						

Table 3. Selected bond distances and angles in segerstromite

As1—O1 (Å)	1.698(2)
—O2	1.679(1) ×3
Ave.	1.684
As2—O3 (Å)	1.776(1) ×3
Ca —O1 (Å)	2.430(1) ×2
—O2	2.381(1) ×2
—O2	2.932(1) ×2
—O3	2.448(1) ×2
Ave.	2.548
O3—H....O2 (Å)	2.664(2)
O3—H (Å)	0.78(2)
∠O3—H....O2 (°)	177(2)

Table 5. Calculated bond-valence sums for segerstromite.

	O1	O2	O3	Sum
Ca	0.286 x 2	0.327 x 2 0.074 x 2	0.272 x 2→	1.918
As1	1.279	1.345 x 3→		5.161
As2			1.035 x 3→	3.104
Sum	1.851	2.146	1.307	

Table 6. Minerals containing both As^{5+} and As^{3+} as essential components.

Mineral name	Chemical formula
Segerstromite	**$Ca_3(AsO_4)_2[As(OH)_3]_2$**
Arakiite	$Zn^{2+}Mn^{2+}_{12}Fe^{3+}_2(As^{3+}O_3)(As^{5+}O_4)_2(OH)_{23}$
Carlfrancisite	$Mn^{2+}_3(Mn^{2+},Mg,Fe^{3+},Al)_{42}[As^{3+}O_3]_2(As^{5+}O_4)_4[(Si,As^{5+})O_4]_6[(As^{5+},Si)O_4]_2(OH)_{42}$
Dixenite	$Cu^{1+}Mn^{2+}_{14}Fe^{3+}(As^{3+}O_3)_5(SiO_4)_2(As^{5+}O_4)(OH)_6$
Hematolite	$(Mn^{2+},Mg,Al)_{15}(As^{3+}O_3)(As^{5+}O_4)_2(OH)_{23}$
Mcgovernite	$Mn^{2+}_{19}Zn^{2+}_3(As^{3+}O_3)(As^{5+}O_4)_3(SiO_4)_3(OH)_{21}$
Radovanite	$Cu^{2+}_2Fe^{3+}(As^{3+}O_2OH)_2(As^{5+}O_4)\cdot H_2O$
Synadelphite	$Mn^{2+}_9(As^{3+}O_3)(As^{5+}O_4)_2(OH)_9\cdot 2H_2O$
Vicanite-(Ce)	$(Ca,Ce,La,Th)_{15}As^{5+}(As^{3+},Na)_{0.5}Fe^{3+}_{0.7}Si_6B_4(O,F)_{47}$

Table 7. Tentative assignments of major Raman bands for segerstromite

Bands (cm^{-1})	Assignment
2906	O-H stretching vibration
2449	Stretching vibration of the strongly hydrogen-bonded OH in the $As(OH)_3$ unit (Frost et al. 2011)
790-910	As^{5+}-O stretching vibrations within the AsO_4 group
610-750	As^{3+}-O stretching vibrations within the $As(OH)_3$ groups
300-500	O-As^{5+}-O and O-As^{3+}-O bending vibrations within AsO_4 and $As(OH)_3$ groups
<300	Lattice and Ca-O vibrational modes